Author Manuscript

Author Manuscript

Author Manuscript

Author Manuscript

HHS Public Access

Author manuscript

Arthritis Rheumatol. Author manuscript; available in PMC 2023 March 08.

Published in final edited form as:

Arthritis Rheumatol. 2016 August ; 68(8): 1989–2002. doi:10.1002/art.39655.

Toll-like Receptor 9 Signaling Is Augmented in Systemic Sclerosis and Elicits Transforming Growth Factor β–Dependent Fibroblast Activation

Feng Fang[#1], **Roberta Goncalves Marangoni**[#1], **Xingchun Zhou**[2], **Yang Yang**[2], **Boping Ye**[2], **Anna Shangguang**[1], **Wenjie Qin**[3], **Wenxia Wang**[1], **Swati Bhattacharyya**[1], **Jun Wei**[1], **Warren G. Tourtellotte**[1], **John Varga**[1]

[1]Northwestern University Feinberg School of Medicine, Chicago, Illinois

[2]China Pharmaceutical University, Nanjing, China

[3]University of Illinois at Chicago, Chicago, Illinois.

[#] These authors contributed equally to this work.

Abstract

Objective.—Although transforming growth factor β (TGFβ) is recognized as being a key trigger of fibroblast activation in systemic sclerosis (SSc), prominent innate immunity suggests that additional pathways contribute to disease persistence. Toll-like receptor 9 (TLR9) is implicated in autoimmunity and fibrosis; however, the expression, mechanism of action, and pathogenic role of TLR9 signaling in SSc remain uncharacterized. The aim of this study was to explore the expression, activity, and potential pathogenic role of TLR9 in the context of skin fibrosis in SSc and in mouse models of experimental fibrosis.

Methods.—Expression and localization of TLR9 were evaluated in SSc skin biopsy specimens and explanted skin fibroblasts. Fibrotic responses elicited by type A CpG oligonucleotide and mitochondrial DNA (mtDNA) were examined in human skin fibroblasts by a combination of real-time quantitative polymerase chain reaction, Western blot analysis, transient transfection, immunofluorescence microscopy, and functional assays. Expression of TLR9 was examined in 2 distinct mouse models of experimental fibrosis.

Results.—Skin biopsy specimens obtained from 2 independent cohorts of SSc patients showed up-regulation of TLR9, and myofibroblasts were the major cellular source. Moreover, SSc skin biopsy specimens showed evidence of TLR9 pathway activation. CpG induced robust TLR9-dependent fibrotic responses in explanted normal fibroblasts that could be blocked by bortezomib

Address correspondence to John Varga, MD, Division of Rheumatology, Feinberg School of Medicine, Northwestern University, McGaw Pavillion M230, 240 East Huron Street, Chicago, IL, 60611. j-varga@northwestern.edu.

AUTHOR CONTRIBUTIONS

All authors were involved in drafting the article or revising it critically for important intellectual content, and all authors approved the final version to be published. Dr. Varga had full access to all of the data in the study and takes responsibility for the integrity of the data and the accuracy of the data analysis.

Study conception and design. Fang, Marangoni, Ye, Tourtellotte, Varga.

Acquisition of data. Fang, Marangoni, Zhou, Yang, Shangguang, Qin, Wang, Bhattacharyya, Wei, Varga.

Analysis and interpretation of data. Fang, Marangoni, Zhou, Yang, Ye, Shangguang, Qin, Wang, Bhattacharyya, Wei, Tourtellotte, Varga.

Author Manuscript Author Manuscript Author Manuscript Author Manuscript

and were mediated through the action of endogenous TGFβ. Mice with experimental fibrosis showed a time-dependent increase in TLR9 localized primarily to myofibroblasts in the dermis.

Conclusion.—In isolated fibroblasts, TLR9 elicits fibrotic responses mediated via endogenous TGFβ. In patients with SSc, mtDNA and other damage-associated TLR9 ligands in the skin might trigger localized activation of TLR9 signaling, TGFβ production, and consequent fibroblast activation. Disrupting this fibrotic process with inhibitors targeting TLR9 or its downstream signaling pathways might therefore represent a novel approach to SSc therapy.

Progressive organ fibrosis due to prolonged fibroblast activation accounts for the intractable nature and high mortality of systemic sclerosis (SSc) (1). By stimulating collagen synthesis and myofibroblast differentiation, transforming growth factor β (TGFβ) plays a key role in SSc pathogenesis (2). In SSc skin biopsy specimens, TGFβ pathway activation has been shown to be strongly correlated with the severity of skin involvement (3–5). However, the mechanisms accounting for aberrant TGFβ production and persistent fibrosis in SSc are not well understood. Expression profiling in SSc skin biopsy specimens reveals evidence of on-going activation of the innate immune system (6,7). Molecular signatures composed of inflammatory chemokines and cytokines, along with interferons (IFNs), coexist with evidence of TGFβ pathway activation in SSc tissue, underscoring the potential involvement of innate immunity in fibrosis (3,8). Innate immunity is triggered by microbial and endogenous (damage-associated) ligands that are recognized through Toll-like receptors (TLRs) expressed on both immune and nonimmune cells. The endosomal pathogen sensor TLR9 recognizes nucleic acids and plays vital roles in antiviral defenses (9). Although the expression and function of TLR9 on immune cells have been characterized extensively, its expression and signaling in nonimmune cells remain poorly characterized despite accumulating evidence of the importance of TLR9 in disease pathogenesis (6).

Of particular interest is the expression and functional role of TLR9 in the context of fibrosis and SSc (6). TLR9 is not present at the cell surface; rather, it is synthesized in the endoplasmic reticulum (ER) in an inactive form, which upon cell activation trafficks through the Golgi complex to endosomal compartments, where it undergoes proteolytic cleavage (10). TLR9 is the only member of the TLR family that is capable of recognizing unmethylated CpG motifs preferentially found in bacterial DNA and much less commonly in mammalian (self) DNA, including mitochondrial DNA (mtDNA) (11). Recent studies show that the γ-herpesvirus Epstein-Barr virus (EBV), which is known to interact directly with TLR9 to trigger antiviral host immunity (12), can be detected within fibroblasts and endothelial cells in SSc skin biopsy specimens (13). In addition to recognizing microbial and viral CpG motifs, TLR9 also recognizes (and is activated by) signals originating from injured or dying mammalian cells, most prominently mtDNA as well as high mobility group box chromosomal protein 1 (HMGB-1) and osteopontin (14). These damage-associated endogenous TLR9 ligands are generated at sites of (sterile) tissue injury and have been implicated as pathogenic danger signals in systemic lupus erythematosus and other autoimmune diseases (15). In light of putative roles of TLR9 in disease pathogenesis, a variety of strategies for therapeutically targeting the TLR9 signaling axis are currently being actively investigated (16).

Author Manuscript Author Manuscript Author Manuscript Author Manuscript

In the current study, we sought to explore the expression, activity, and potential pathogenic role of TLR9 in the context of skin fibrosis in SSc and in mouse models of experimental fibrosis. Our results show that TLR9 is constitutively expressed and functional in isolated normal and SSc fibroblasts and is up-regulated and colocalizes with myofibroblasts in SSc skin biopsy specimens. Moreover, skin fibrosis induced in the mouse by 2 distinct experimental approaches is accompanied by accumulation of TLR9-positive myofibroblasts within the lesional dermis. Treatment of skin fibroblasts with synthetic TLR9 agonists elicits robust fibrotic responses, including up-regulation of collagen synthesis and myofibroblast transformation. These TLR9-mediated profibrotic effects in fibroblasts involve the autocrine actions of TGFβ and can be blocked by the proteasome inhibitor bortezomib, pharmacologic CpG antagonists, or interference RNA (RNAi)–mediated disruption of TLR9 pathways, as well as by blockade of TGFβ signaling. Taken together, our findings provide strong evidence supporting a pathogenic role of TLR9 in fibrotic skin disease and suggest that blocking TLR9-mediated fibrotic responses might be a novel approach for therapeutic control of the process in SSc.

MATERIALS AND METHODS

Cell culture and reagents.

Primary cultures of fibroblasts were established by explantation from neonatal foreskin biopsy specimens or lesional skin biopsy specimens obtained from patients with SSc, under protocols approved by the Institutional Review Boards of Northwestern University and Boston University. Primary fibroblasts and mouse NIH3T3 cells were maintained in Dulbecco's modified Eagle's medium (DMEM) supplemented with 10% fetal bovine serum (FBS) (Lonza), 50 μg/ml penicillin, and 50 μg/ml streptomycin in a humidified atmosphere of 5% CO_2 at 37°C and studied between passages 2 and 8. At early confluence, medium with 0.1% FBS or serum-free medium with 0.1% bovine serum albumin (BSA) was added to the cultures, followed 24 hours later by type A CpG (CpG-A) oligonucleotide 2216 (InvivoGen) or TGFβ2 (PeproTech). In selected experiments, myeloid differentiation factor 88 (MyD88)–blocking peptides (catalog no. tlrl-pimyd), BAY11–7085, and inhibitory CpG (iCpG; catalog no. tlrl-ttag) (all from InvivoGen), SB431542 (GlaxoSmithKline), anti-TGFβ antibodies (R&D Systems), LY294002 (Cell Signaling Technology), U0126 (Cell Signaling Technology), or bortezomib (Millennium Pharmaceuticals) was added to the cultures 60–120 minutes prior to the addition of CpG. Mitochondrial DNA was prepared from normal fibroblasts, using commercial reagents and methods as described by the manufacturer (BioVision) (17), and added to confluent cultures. Cytotoxicity was determined using an LDH-Cytotoxicity Assay Kit (BioVision).

RNA isolation and real-time quantitative polymerase chain reaction (qPCR).

At the end of the experiments, cultures were harvested, and RNA was isolated using an RNeasy Plus Mini Kit (Qiagen) and examined by real-time qPCR (18).

Transient transfection assays.

Fibroblasts at early confluence were transfected with PAI1-Luc, CoL1A2-Luc, ASMA-Luc, or SBE4-Luc plasmids using SuperFect Transfection kits (Qiagen) (19). Cultures

Author Manuscript Author Manuscript Author Manuscript Author Manuscript

were preincubated in serum-free medium containing 0.1% BSA with iCpG (5 μg/ml) for 120 minutes, followed by CpG (5 μg/ml) for 24 hours. Whole cell lysates were assayed for their luciferase activities (Promega). In each experiment, *Renilla* luciferase pRL-TK (Promega) was cotransfected as control for transfection efficiency (20). Transient transfection experiments were performed in triplicate and repeated at least twice, and consistent results were observed.

Determination of TGFβ levels and activity in fibroblast cultures.

Supernatants from confluent cultures incubated in serum-free medium with CpG (5 μg/ml) or mtDNA for the indicated periods of time were stored at −80°C. Levels of TGFβ were determined by enzyme-linked immunosorbent assays performed in triplicate (R&D Systems). To determine levels of active TGFβ generated by CpG-stimulated fibroblasts, plasminogen activator inhibitor 1 (PAI-1) assays were used (21). Briefly, conditioned media were added to cultures of mink lung epithelial cells stably transfected with human PAI1-Luc constructs (a gift from Dr. William Schnaper, Northwestern University, Chicago, Illinois) (21). Following 24-hour incubation, whole cell lysates were prepared and assayed for their luciferase activities.

Confocal immunofluorescence microscopy.

Fibroblasts (10,000/well) were seeded onto 8-well Lab-Tek II Chamber Slides (Nalge Nunc International) and preincubated in serum-free DMEM with iCpG (5 μg/ml) for 120 minutes followed by CpG (5 μg/ml) for a further 24 hours. At the end of the experiments, cells were fixed, permeabilized, incubated with primary antibodies against pSmad3 at 1:200 dilution (Cell Signaling Technology), TLR9 (Abcam) at 1:200 dilution, type I collagen (SouthernBiotech) at 1:500 dilution, or ASMA (Sigma) at 1:500 dilution, followed by secondary antibodies at 1:200 dilution (Alexa Fluor 488 and Alexa Fluor 594; Invitrogen). Images were captured under a Nikon C2 or A1Si confocal microscope and quantitated using ImageJ (National Institutes of Health).

Western blot analysis.

At the end of the experiments, fibroblast cultures were harvested, and whole cell protein lysates were subjected to Western blot analysis. The following antibodies were used: anti–type I collagen (SouthernBiotech), anti–α-smooth muscle actin (anti–α-SMA) (Sigma), anti-GAPDH (Zymed), and anti–α-tubulin (Sigma). Bands were visualized using enhanced chemiluminescence reagents (Pierce), and images were captured using a Fujifilm (Fuji). In each sample, band intensities were quantified with ImageJ software and normalized to GAPDH.

In vitro wound-healing and gel contraction assays.

Fibroblasts were seeded onto 6-well plates. Pipette tips were used to make a scratch in confluent cultures, followed by incubation in medium with CpG (5 μg/ml) for 24 hours. The width of the scratch was imaged at the indicated intervals and measured using ImageJ. To determine the effects of CpG on fibroblast contractility, in vitro collagen gel contraction assays were performed (22). Briefly, fibroblasts were seeded onto 12-well plates (10^6 cells/

Author Manuscript Author Manuscript Author Manuscript Author Manuscript

well) in DMEM with 10% FBS and type I collagen (3.8 mg/ml; BD Biosciences). Collagen gels were allowed to polymerize and were then incubated in medium with TGFβ (10 ng/ml) in the presence or absence of CpG (5 μg/ml) for up to 6 days. The extent of gel contraction was measured at the indicated intervals, and the percentage of the gel diameter compared with control was calculated. Each experiment was performed in triplicate.

Immunohistochemistry and immunofluorescence.

To assess TLR9 expression in skin, biopsy specimens obtained from the affected forearms of SSc patients in 2 independent cohorts were studied. The first cohort consisted of patients with early-stage (<13 months from the first non-Raynaud's manifestation) diffuse cutaneous SSc (n = 8) or healthy adult subjects (n = 4). The biopsy specimens were examined by immunohistochemistry. The biopsy specimens were obtained under protocols approved by the Institutional Review Boards for human studies at Boston University (additional information is available upon request from the corresponding author). Paraffin-embedded tissue sections (5 μm thick) were immunostained with primary antibody to TLR9 (Cell Signaling Technology) followed by horseradish peroxidase–labeled secondary antibody (Invitrogen) and counterstained with hematoxylin. Preincubation with nonimmune serum served as negative control. Images were acquired on a Zeiss Axioskop microscope with a CRi Nuance spectral camera. TLR9 levels were determined by calculating the percentage of TLR9-immunopositive cells within the dermis. Cells were counted in 5 randomly selected high-power fields (hpf) per biopsy specimen by an observer in a blinded manner.

A second independent cohort of SSc patients with early-stage disease (≤24 months from the first non-Raynaud's manifestation), patients with late-stage disease, and healthy controls was used for validation. Biopsy specimens were obtained under protocols approved by the Institutional Review Boards for human studies at Northwestern University (additional information is available upon request from the corresponding author). Skin biopsy specimens were examined by the double-label technique using antibodies against TLR9 and α-SMA (both from Abcam) as well as DAPI to identify nuclei. Negative control specimens stained without primary antibody were used to confirm specificity. Images were acquired on a Nikon A1R laser scanning confocal microscope. TLR9 and α-SMA levels in the skin were determined by scoring TLR9- and α-SMA–immunopositive cells and total nuclei in 3 randomly selected hpf throughout the dermis. Cells with distinct capillary morphology were excluded from the analysis.

To examine changes in TLR9 expression in vivo, fibrosis was induced in mice, using 2 experimental approaches. First, 6–8-week-old female C57BL/6 mice (The Jackson Laboratory) received bleomycin via daily subcutaneous injections (1 mg/kg) (23,24). In a complementary approach, mice were administered AdTGFβ1$^{223/225}$ or adenovirus expressing LacZ protein (AdLacZ) (from Dr. Jack Gauldie, McMaster University, Ontario, Quebec, Canada) (25) via a single subcutaneous injection and killed 42 days later. All animal protocols were institutionally approved by the Northwestern University Animal Care and Use Committee. Each experimental group consisted of at least 4 mice. At the end of the experiments, the mice were killed, lesional skin was harvested, and double immunofluorescence analysis using antibodies against TLR9 (Abcam), α-SMA (Abcam), or

Author Manuscript Author Manuscript Author Manuscript Author Manuscript

F4/80 (eBioscience) was performed, followed by incubation with Alexa Fluor–conjugated IgG secondary antibodies (Invitrogen) (26). Sections were imaged at 400× magnification at 4 different hpf spanning the dermis under a Nikon A1R laser scanning confocal microscope. IgG was used as negative control. Immunopositive interstitial cells within the lesional dermis were counted by an observer who was blinded to treatment. The proportion of cells with double staining (protein of interest plus marker protein) was determined by calculating the ratio of double-positive cells to single-positive cells in at least 3 hpf per mouse.

TLR9-responsive gene signature in SSc skin biopsy specimens.

An experimentally derived TLR9 gene signature was established based on microarray data (GEO accession no. GSE30849) from human plasmacytoid dendritic cells (PDCs) treated with CpG for 24 hours. Microarray expression data for SSc skin biopsy specimens were obtained (GEO accession nos. GSE9285 and GSE32413) (27,28). The TLR9 signature was defined by the set of genes showing ≥1.5-fold up-regulation or down-regulation in response to CpG stimulation (false discovery rate ≤0.05). Enrichment analyses of Gene Ontology (GO) biologic processes and Kyoto Encyclopedia of Genes and Genomes (KEGG) pathways were performed using DAVID (29). The experimentally derived TLR9 gene signatures were mapped to skin biopsy specimen microarray data. Expression values for each probe in the patient data sets were centered to the median values across all samples. Probes were filtered due to small variance across all samples. Average linkage hierarchical clustering was performed on samples using the uncentered Pearson's correlation coefficient (30). Significance of clustering was determined using SigClust (31). Pearson's correlation coefficient was then calculated to determine the correlation between the TLR9 gene signature and intrinsic subsets. The statistical significance of the difference in the correlation coefficient between 2 groups was determined by 2-sided *t*-test. All analyses and heatmap visualizations were carried out using the R software package (http://www.r-project.org/).

Statistical analysis.

Statistical analysis was performed in Microsoft Excel or GraphPad Prism 6 using Student's *t*-test, the Wilcoxon-Mann-Whitney test, or analysis of variance. Results are shown as the mean ± SEM. *P* values less than 0.05 were considered significant.

RESULTS

Increased TLR9 expression in SSc.

Skin biopsy specimens obtained from the forearms of healthy subjects and patients with SSc were examined by immunohistochemistry and immunofluorescence (additional information is available upon request from the corresponding author). In the epidermis, TLR9 expression was comparable between healthy control subjects and patients with SSc; in the dermis, TLR9 expression was significantly elevated in patients with SSc compared with controls (Figures 1A and B). Both patients with early-stage and those with late-stage disease showed increased TLR9 expression in the skin. Double-label immunofluorescence analysis indicated that >60% of the α-SMA–positive myofibroblasts in the fibrotic dermis in patients with SSc were TLR9 positive (Figure 1C). Among patients with dcSSc (n = 10), the proportion of TLR9-positive myofibroblasts was greater in those with late-stage disease compared with

Author Manuscript Author Manuscript Author Manuscript Author Manuscript

those with early-stage disease ($P = 0.03$) (additional information is available upon request from the corresponding author).

When grown in monolayers, skin fibroblasts isolated from healthy donors and patients with SSc showed detectable messenger RNA (mRNA) transcripts for all 10 TLRs in culture (additional information is available upon request from the corresponding author). Expression of TLR9, which in skin fibroblasts was relatively low compared with TLR4 expression (<1%), was >3-fold higher in SSc fibroblasts (n = 4) compared with that in fibroblasts from healthy controls (n = 4) (Figure 1C). Intact TLR9 signaling in these cells was functionally confirmed by incubation with the TLR9 ligand CpG, which elicited potent time-dependent induction of interleukin-6 (IL-6) and other classic TLR9 target genes.

TLR9 gene signature in SSc skin biopsy specimens.

To seek evidence of TLR9 activation in SSc skin, an experimentally derived TLR9 gene signature was generated using publicly available microarray data (see Materials and Methods) (32). A total of 1,054 unique genes showed a ≥1.5-fold change (up or down) in response to CpG, with 92% of these genes (974 of 1,054) showing the same directionality of changes induced by all tested CpG isoforms (32). This 974-gene TLR9 signature included known TLR9-regulated genes including CXCL10, CCL4, TNF, and IFNA (additional information is available upon request from the corresponding author). GO and KEGG pathway analysis showed enrichment of the experimentally derived TLR9 signature with genes that are involved with immunity, antiviral responses, and immune responses.

To determine the implications of activated TLR9 signaling in the context of SSc, we quantitated the TLR9 gene signature in skin biopsy specimens. For this purpose, we queried a genome-wide microarray data set comprising lesional and nonlesional skin biopsy specimens from 27 SSc patients and 6 healthy control subjects (27,28). Data for TLR9-responsive genes (a total of 314 genes representing 388 probes) were extracted from the data set (Figure 2) (additional information is available upon request from the corresponding author). A heatmap of the 75 biopsy microarray data was generated using intrinsic gene clustering (27,28), and the level of enrichment with the 314-gene TLR9 signature in each sample was quantified. Significant enrichment with the TLR9 signature was seen in skin biopsy specimens clustering with the inflammatory intrinsic subsets compared with all other samples (r = 0.2). The inflammatory intrinsic subset comprises 5 distinct gene clusters (groups). Gene expression levels in cluster 1 in this inflammatory intrinsic subset showed no significant difference from the levels in genes in the normal-like intrinsic subset, but the expression levels were increased in the diffuse 1 and diffuse 2 subsets. Gene expression levels in cluster 2 in the inflammatory intrinsic subset were higher than the levels of genes in the normal-like intrinsic subset. This cluster of genes was enriched with antigen processing, immune response, and defense response functions by GO analysis (Figure 2).

Elicitation of TLR9-dependent fibrotic responses by CpG-A oligonucleotides.

Because SSc skin biopsy specimens showed both elevated TLR9 expression and evidence of active TLR9 signaling, we sought to examine the effects of TLR9 on fibroblast responses. Incubation of healthy skin fibroblasts with the synthetic TLR9 ligand CpG-A elicited dose-

Author Manuscript Author Manuscript Author Manuscript Author Manuscript

dependent stimulation of COL1A1, COL1A2, ASMA, PAI1, and COMP mRNA expression and increased the levels of type I collagen (Figures 3A–C and results not shown). Moreover, CpG treatment induced an increase in ASMA accumulation within cytoplasmic stress fibers, a hallmark of mature myofibroblasts (Figure 3C). Expression of TLR9 mRNA was also stimulated by CpG (1.5 fold; $P < 0.05$) (data not shown). To examine the effects of TLR9 activation on fibroblast contractility, cells seeded in collagen gels were incubated in medium with CpG and/or TGFβ for up to 6 days. CpG by itself potently stimulated gel contraction and significantly enhanced the effect of TGFβ (Figure 3D). Additionally, in vitro wound-healing assays showed that CpG markedly augmented fibroblast migration (Figure 3E).

To determine the role of TLR9 in mediating the fibrotic responses elicited by CpG, a series of complementary strategies was used. Small interfering RNA–mediated TLR9 knockdown, which caused a >80% decrease in cellular TLR9, was accompanied by abrogation of CpG-induced fibrotic gene expression (Figure 4C). Pretreatment of cultures with iCpG, which binds to the TLR9 extracellular domain but is unable to activate signaling (33), prevented CpG-induced fibrotic responses in a dose-dependent manner, and disrupted canonical TGFβ/Smad signaling (Figures 4D and E and results not shown) (additional information is available upon request from the corresponding author). These inhibitory effects of iCpG occurred in the absence of detectable cytotoxicity.

Full-length TLR9 within the ER is nonfunctional and inactive. Nascent TLR9 must be delivered into the endolysosomes, where it undergoes proteolytic cleavage to generate the functional active receptor (34,35). Bortezomib is a selective inhibitor of the 26S proteasome that is currently approved for the treatment of multiple myeloma (36). Bortezomib has been shown to have pro-found effects on ER homeostasis (37) and can block CpG-induced trafficking of TLR9 from the ER to endolysosomes (38). Pretreatment of fibroblasts with bortezomib abrogated CpG-induced stimulation of collagen and ASMA expression (additional information is available upon request from the corresponding author). Taken together, these results establish an essential functional role for TLR9 in mediating the profibrotic effects of CpG. To delineate the intracellular pathways involved in these responses, cultures were pretreated with inhibitors of MyD88 (pMyD88) or NF-κB (BAY11–7082), which sequentially block canonical TLR9 signaling (39). Both compounds potently inhibited COL1A1 and ASMA in CpG-treated cultures while effectively blocking stimulation of IFNA1 and IL-6, as expected (Figures 4A and B and data not shown) (additional information is available upon request from the corresponding author).

Mediation of TLR9-dependent fibrotic responses by endogenous TGFβ.

In light of the fundamental role that TGFβ plays in orchestrating fibrogenesis in vivo, we sought to evaluate its regulation by TLR9 and its role in fibrotic responses. CpG treatment of normal fibroblasts induced an early and transient increase in IFN gene expression, peaking at 4 hours, followed by a decline to basal levels (Figure 5B). Subsequently, a progressive and sustained increase in TGFβ expression was noted, which preceded the increase in COL1A1 and ASMA expression (Figures 5A and B). Time-dependent induction of fibrotic responses by CpG was blocked by neutralizing anti-TGFβ antibodies as well as a small-molecule inhibitor of the canonical Smad pathway (Figures 5C and D). Moreover,

Author Manuscript Author Manuscript Author Manuscript Author Manuscript

CpG treatment elicited increased Smad3 phosphorylation and nuclear accumulation (Figure 5E). Cell-free conditioned medium from CpG-treated cultures elicited marked simulation of PAI1-Luc activity, indicating the presence of activated TGFβ in the supernatants (Figure 5F). Incubation of fibroblasts with mtDNA, an endogenous TLR9 ligand, resulted in significant up-regulation of TGFβ levels, which was completely abrogated by pretreatment of the cultures with iCpG (Figure 5G). Collectively, these results identified production and activation of endogenous TGFβ as being critical mechanisms underlying TLR9-dependent fibrotic responses.

Association between elevated TLR9 expression and skin fibrosis in murine scleroderma.

To investigate the regulation of TLR9 in experimental fibrogenesis, lesional skin from mice treated with PBS, bleomycin, AdTGF-$\beta 1^{223/225}$, or AdLacZ was harvested. Bleomycin injections induced a cutaneous inflammatory response by days 3–5, and significant dermal fibrosis was observed by day 14. Elevated levels of TLR9 mRNA in the lesional skin were seen early (days 3–5) and persisted until day 21 (data not shown). In PBS-treated mice, TLR9-positive cells were observed primarily in the epidermis and were scant-to-absent within the dermis (Figure 6).

Bleomycin caused a time-dependent increase in the number of TLR9/positive cells in the skin that peaked on day 21, with the most prominent accumulation seen within the reticular dermis. With progression of dermal fibrosis, an increasing proportion of α-SMA–positive interstitial myofibroblasts expressed TLR9, while the proportion of F4/80-positive macrophages coexpressing TLR9 declined at the later time points (Figure 6A). To examine changes in cutaneous TLR9 expression in an alternate model of experimental skin fibrosis, we administered single subcutaneous injections of AdTGFβ1 or AdLacZ (as a negative control) to 6–8-week-old mice, and their skin was harvested 6 weeks later. AdTGFβ1 induced an almost 3-fold increase in TLR9 expression ($P = 0.0001$) within the lesional dermis (Figure 6B).

Taken together with our observations in SSc biopsy specimens (Figure 1), these findings indicated that skin fibrosis in SSc and in mice is accompanied by up-regulation of TLR9 on myofibroblasts within the lesional dermis, suggesting that TLR9-dependent activation of these stromal cells might contribute to the progression of skin fibrosis in patients with SSc and in mice with experimentally induced scleroderma.

DISCUSSION

Although both innate immunity and TGFβ-mediated fibrotic responses are implicated in the pathogenesis of SSc, the precise mechanisms and mediators regulating the cross-talk between these processes in the context of fibrosis remain incompletely understood (6). The results of the current study indicate that fibroblast activation mediated through the endosomal pathogen sensor TLR9 might be an important factor contributing to the progression of skin fibrosis in SSc. Our results reveal that TLR9 levels are elevated in the skin of patients with SSc and in mouse models of cutaneous fibrosis and colocalize with myofibroblasts. Furthermore, lesional SSc skin biopsy specimens show TLR9-regulated gene expression signatures, suggesting on-going TLR9 pathway activation. In isolated skin

Author Manuscript Author Manuscript Author Manuscript Author Manuscript

fibroblasts, TLR9 activation by CpG elicits early inflammatory and subsequent profibrotic responses, including the production of activated TGFβ, which participate in an autocrine fibrosis amplification loop. Coexpression of the TGFβ- and TLR9-driven molecular signatures in the same SSc skin biopsy specimens lends support for implicating TLR9 in both inflammation and TGFβ-driven tissue fibrosis. Targeting aberrant TLR9 signaling in SSc using TLR9 inhibitors might therefore represent a novel strategy for halting the progression of fibrosis, particularly in patients whose skin biopsy specimens show evidence of activated innate immunity.

TLRs on both immune and nonimmune cells represent the first line of defense against microbial pathogens but are also increasingly being implicated in the progression of chronic autoimmune and fibrotic diseases (11). Our results indicate that TLR9 is expressed and functional in both normal and SSc skin fibroblasts, and its expression is elevated in myofibroblasts in SSc skin biopsy specimens, most prominently in patients with late-stage disease. This suggests that persistent TLR9 expression might be causally linked to persistent myofibroblast activation and might be a factor accounting for the failure to resolve fibrosis in these patients. The expression of TLR9 in a variety of cell types is enhanced by TGFβ as well as CpG (40), while its intracellular trafficking from the ER into the endolysosome and biologic activities are regulated by a variety of factors (34,41,42). Elevated expression of TLR9 has been demonstrated previously in the lungs of patients with idiopathic pulmonary fibrosis (IPF), where its levels were shown to correlate with rapid disease progression (43). The question of whether increased TLR9 expression in SSc skin correlates with disease severity or activity, or can predict disease progression, awaits further study.

A TLR9-responsive gene signature was generated and used to analyze a microarray expression data set from SSc and healthy skin biopsy specimens (27,28). The TLR9 gene signature showed considerable overlap with the signature generated in mice via long-term TLR9 activation by CpG injection of the skin (44). The TLR9 gene signature was highly expressed in 7 SSc skin biopsy specimens and showed a strong association with the inflammatory intrinsic gene expression subset. Co-occurrence of TLR9 pathway activation with the TGFβ gene signature in SSc skin (3) is consistent with a model of TLR9 activation in the lesional tissue driving local TGFβ production, which is in turn responsible for increased collagen synthesis, myofibroblast differentiation, and related profibrotic responses.

To investigate the effects of TLR9 activation in skin fibroblasts as primary effector cells in SSc (45), we used synthetic DNA fragments containing an immunomodulatory CpG motif. In normal fibroblasts, CpG treatment caused increased collagen production and myofibroblast transformation accompanied by increased fibroblast contractility and migration. An indispensable role for cellular TLR9 in mediating these profibrotic responses was established by a combination of RNAi, competitive inhibitors, and an MyD88 inhibitor, while disruption of intracellular TLR9 trafficking using the proteasome inhibitor bortezomib provided further evidence that fibrotic CpG signaling requires the mature form of endosomal TLR9. Consistent with the inhibitory effects of bortezomib on profibrotic TLR9 signaling, we showed in previous work that bortezomib attenuated bleomycin-induced skin and lung fibrosis in mice (46).

Author Manuscript Author Manuscript Author Manuscript Author Manuscript

The current study indicates that TLR9 activation resulted in robust and sustained production of TGFβ, which in turn induced intracellular Smad2/3 activation in an autocrine manner. Significantly, the increase in TGFβ mRNA in CpG-treated fibroblasts followed the self-limited burst of IFN production but preceded the increase in COL1A1 mRNA. Blocking TGFβ signaling using either neutralizing antibodies or a small-molecule inhibitor of Smad2/3 phosphorylation abolished the profibrotic effects of CpG, indicating that TLR9-dependent stimulation of collagen gene expression involved endogenous TGFβ. It is noteworthy that although CpG induced TGFβ production, TGFβ itself is a potent stimulus of increased TLR9 expression and activation in normal lung fibroblasts (40). Moreover, TGFβ also promotes proteolytic cleavage of TLR9 to the 80–90-kd biologically active form. In this way, a positive feedback loop might be established in which TLR9 activity in fibroblasts leads to production of TGFβ, which in turn drives enhanced TLR9 expression and activity. This self-amplifying loop might account for the failure to appropriately restrict a transient and normally self-limiting TLR9 response to tissue injury. Therefore, in the setting of excess TGFβ levels within the cellular milieu in SSc, unchecked long-term TLR9 signaling is likely to contribute to progressive fibrosis.

The putative endogenous ligands that might be responsible for eliciting fibroblast TLR9 signaling in fibrotic conditions are not well characterized. The γ-herpesviruses such as EBV and Kaposi's sarcoma–associated herpesvirus can interact directly with TLR9 (12). The intriguing possibility that EBV reactivation might provide a self-ligand for TLR9 activation in fibrosis was suggested by recent observations of EBV detection in the lungs of patients with IPF (47) and SSc skin biopsy specimens (13). However, the causal role of herpesvirus-mediated TLR9 activation in fibrosis remains to be experimentally validated. Importantly, TLR9 can also be activated by endogenous damage–associated ligands generated during tissue injury and apoptotic or necrotic cell death (11).

Whether TLR9 in lesional SSc skin fibroblasts might become activated in response to damage-associated molecular patterns such as HMGB-1, osteopontin, or mtDNA generated within lesional skin micro-environments remains to be investigated. Mitochondrial DNA was recently shown to be a potent endogenous inducer of TLR9 signaling (48,49). It is therefore of substantial interest that mice with bleomycin-induced scleroderma show mitochondrial dysfunction and release mtDNA (50). Moreover, isolated SSc skin fibroblasts show evidence of spontaneous mitochondrial reactive oxygen species generation and accumulation of mtDNA (Bhattacharyya S, et al: unpublished observations).

We observed that treatment of normal fibroblasts with mtDNA elicited TLR9-dependent stimulation of TGFβ, which is consistent with a potential role of damage-associated mtDNA as an endogenous TLR9 ligand driving TGFβ production. Osteopontin, an endogenous TLR9 ligand (51), was recently shown to be up-regulated in the skin of SSc patients and bleomycin-treated mice (52). In addition, it is also possible that TLR9 is constitutively activated in SSc, because TGFβ-driven intracellular cleavage and maturation of TLR9 result in its export from the ER in the absence of ligand activation (40). This intriguing possibility remains to be investigated.

Author Manuscript Author Manuscript Author Manuscript Author Manuscript

An early increase in the number of TLR9-positive macrophages in the skin of mice with bleomycin-induced fibrosis was followed by accumulation of TLR9-expressing myofibroblasts that paralleled the development of fibrosis. Because TLR9 promotes myofibroblast differentiation, we speculate that myofibroblasts within the lesional dermis might originate from TLR9-expressing fibroblasts. The factors responsible for initiating TLR9 up-regulation in these cells cannot be discerned on the basis of the current study. However, because both TGFβ and nucleic acids are known to up-regulate TLR9 in nonimmune cells (40), we surmise that these factors signal the process in experimentally induced scleroderma as well as in patients with SSc. Prolonged TLR9 activation in myofibroblasts then results in sustained local TGFβ production and autocrine fibrosis amplification loops that impede the resolution of fibrosis.

Studies in animal models provide support for a potentially pathogenic role of TLR9 in organ fibrosis. Administration of CpG was shown to enhance TLR9-dependent fibrosis and/or inflammation of the lungs, liver, and skin of mice (43,44,53) and promoted invasive fibroblast phenotypes in models of breast and prostate cancer (54). Mice lacking TLR9 showed attenuation of fibrosis in the liver (53). In contrast to these findings, however, other studies suggest a profibrotic role for TLR9 in vivo, showing exacerbation of lung fibrosis induced by γ-herpesvirus in TLR9-null mice (55) and exaggerated liver fibrosis following chemical injury (56). In these examples, loss of TLR9 was associated with Th2 cell polarization of the immune response and an impaired ability to mount a type 1 immune response. Similarly, TLR9-null mice developed an exaggerated fibrotic/granulomatous response in the lungs upon *Schistosoma mansoni* egg embolization (57). Moreover, a recent study showed that CpG treatment attenuated CCl_4-induced liver fibrosis in C57BL/6 wild-type mice (56). In the TSK/+ mouse model of scleroderma, CpG administration was shown to prevent the development of hypodermal fibrosis, with the antifibrotic effect attributed to increased circulating levels of antifibrotic Th1 cytokines (58). As these studies illustrate, the effects of TLR9 activation in the context of tissue remodeling are complex, with the ultimate outcome depending on the nature and chronicity of the TLR9-activating injury as well as the temporal and spatial balance of profibrotic and antifibrotic effects of TLR9-dependent mediators on the target organ stromal cells.

A limitation of the current study is the absence of studies in mice lacking TLR9. Although our results establish a fibroblast-specific TLR9-dependent profibrotic effect of CpG, whether TLR9 in vivo promotes fibrosis or restricts it cannot be accurately predicted from these cell-based assays despite the obvious clinical relevance. Although the TLR system is generally viewed as being one of relatively low complexity, the biologic outcomes of TLR9 activation are context dependent, determined by the cell type, as well as the nature and dose of activating signal and duration of exposure, as well as other factors. For instance, although low doses of CpG are immunostimulatory and are being exploited as a therapeutic approach, CpG at high doses promotes an opposite tolerogenic response mediated by TGFβ-dependent non-canonical immune suppression (59). TLR9 is expressed on immune cells including B lymphocytes, monocytes, macrophages, natural killer cells, and PDCs, where its activation leads to the generation of inflammatory cytokines, IFNγ, chemokines, and adhesion molecules, with a predominantly Th1 response (60). In the context of tissue remodeling and fibrogenesis, Th1 responses are generally viewed as antifibrotic, suggesting

Author Manuscript Author Manuscript Author Manuscript Author Manuscript

that long-term TLR9 activation in vivo might in fact promote suppression of fibrosis. As discussed above, CpG has been shown to exert both profibrotic and antifibrotic effects in mice, and genetic deletion of TLR9 has likewise been linked to both amelioration and exacerbation of organ fibrosis in experimental mouse models.

In summary, the present study indicates that TLR9 expression and signaling are persistently increased in SSc skin biopsy specimens, and in mice TLR9 is up-regulated in lesional myofibroblasts in experimentally induced models of fibrosis. Ligand-induced TLR9 activation in explanted fibroblasts in culture elicits sustained fibrotic responses that are mediated through autocrine TGFβ signaling. Although the nature of the signals responsible for elevated TLR9 expression in SSc and the pathogenic endogenous ligands driving TLR9-dependent fibroblast activation remain to be firmly established, our results suggest the possibility that TLR9 and its self ligands might play key roles in pathologic skin fibrosis.

ACKNOWLEDGMENTS

We thank Chengning Zhang, Lei Liu, and Wen Hong for technical assistance, and Hui Lu (University of Illinois) and members of the Varga laboratory for helpful discussions.

Supported by the NIH (grants R01-NS-040748 and K26-OD-010945 to Dr. Tourtellotte and grant R01-AR-04239 to Dr. Varga). Imaging was performed at the Northwestern University Center for Advanced Microscopy; histologic analysis was performed at the Northwestern University Mouse Histology and Phenotyping Laboratory. Both are supported by the NIH (National Cancer Institute Cancer Center Support Grant award P30-CA-060553). The Boston University Dermatopathology Core is supported by the NIH (grant AR-061271).

REFERENCES

1. Allanore Y, Simms R, Distler O, Trojanowska M, Pope J, Denton CP, et al. Systemic sclerosis. Nat Rev Dis Primers 2015;1:15002.
2. Bhattacharyya S, Wei J, Varga J. Understanding fibrosis in systemic sclerosis: shifting paradigms, emerging opportunities. Nat Rev Rheumatol 2012;8:42–54.
3. Johnson ME, Mahoney JM, Taroni J, Sargent JL, Marmarelis E,Wu MR, et al. Experimentally-derived fibroblast gene signatures identify molecular pathways associated with distinct subsets of systemic sclerosis patients in three independent cohorts. PLoS one 2015;10:e0114017.
4. Sargent JL, Milano A, Bhattacharyya S, Varga J, Connolly MK,Chang HY, et al. A TGFβ-responsive gene signature is associated with a subset of diffuse scleroderma with increased disease severity. J Invest Dermatol 2010;130:694–705. [PubMed: 19812599]
5. Rice LM, Padilla CM, McLaughlin SR, Mathes A, Ziemek J,Goummih S, et al. Fresolimumab treatment decreases bio-markers and improves clinical symptoms in systemic sclerosis patients. J Clin Invest 2015;125:2795–807. [PubMed: 26098215]
6. Bhattacharyya S, Varga J. Emerging roles of innate immune signaling and toll-like receptors in fibrosis and systemic sclerosis. Curr Rheumat Rep 2015;17:474.
7. Mahoney JM, Taroni J, Martyanov V, Wood TA, Greene CS, Pioli PA, et al. Systems level analysis of systemic sclerosis shows a network of immune and profibrotic pathways connected with genetic polymorphisms. PLoS Comput Biol 2015;11:e1004005.
8. Lafyatis R. Transforming growth factor β: at the centre of systemic sclerosis. Nat Rev Rheumatol 2014;10:706–19. [PubMed: 25136781]
9. Mogensen TH. Pathogen recognition and inflammatory signalingin innate immune defenses. Clin Microbiol Rev 2009;22:240–73, Table of Contents. [PubMed: 19366914]
10. Chockalingam A, Brooks JC, Cameron JL, Blum LK, Leifer CA.TLR9 traffics through the Golgi complex to localize to endolysosomes and respond to CpG DNA. Immunol Cell Biol 2009;87:209–17. [PubMed: 19079358]

Author Manuscript Author Manuscript Author Manuscript Author Manuscript

11. Bryant CE, Gay NJ, Heymans S, Sacre S, Schaefer L, Midwood KS. Advances in Toll-like receptor biology: modes of activation by diverse stimuli. Crit Rev Biochem Mol Biol 2015:50:359–79. [PubMed: 25857820]
12. Guggemoos S, Hangel D, Hamm S, Heit A, Bauer S, Adler H.TLR9 contributes to antiviral immunity during gammaherpesvirus infection. J Immunol 2008;180:438–43. [PubMed: 18097045]
13. Farina A, Cirone M, York M, Lenna S, Padilla C, McLaughlin S, et al. Epstein-Barr virus infection induces aberrant TLR activation pathway and fibroblast-myofibroblast conversion in scleroderma. J Invest Dermatol 2014;134:954–64. [PubMed: 24129067]
14. Kawai T, Akira S. The role of pattern-recognition receptors ininnate immunity: update on Toll-like receptors. Nat Immunol 2010;11:373–84. [PubMed: 20404851]
15. Means TK, Latz E, Hayashi F, Murali MR, Golenbock DT, Luster AD. Human lupus autoantibody-DNA complexes activate DCs through cooperation of CD32 and TLR9. J Clin Invest 2005;115:407–17. [PubMed: 15668740]
16. Gambuzza M, Licata N, Palella E, Celi D, Foti Cuzzola V, Italiano D, et al. Targeting Toll-like receptors: emerging therapeutics for multiple sclerosis management. J Neuroimmunol 2011;239:1–12. [PubMed: 21889214]
17. Negmadjanov U, Godic Z, Rizvi F, Emelyanova L, Ross G, Richards J, et al. TGF-β1-mediated differentiation of fibroblasts is associated with increased mitochondrial content and cellular respiration. PLoS One 2015;10:e0123046.
18. Fang F, Ooka K, Bhattachyya S, Wei J, Wu M, Du P, et al. Theearly growth response gene Egr2 (Alias Krox20) is a novel transcriptional target of transforming growth factor-β that is up-regulated in systemic sclerosis and mediates profibrotic responses. Am J Pathol 2011;178:2077–90. [PubMed: 21514423]
19. Fang F, Ooka K, Sun X, Shah R, Bhattacharyya S, Wei J, et al. Asynthetic TLR3 ligand mitigates profibrotic fibroblast responses by inducing autocrine IFN signaling. J Immunol 2013;191:2956–66. [PubMed: 23956427]
20. Fang F, Antico G, Zheng J, Clevenger CV. Quantification ofPRL/Stat5 signaling with a novel pGL4-CISH reporter. BMC Biotechnol 2008;8:11. [PubMed: 18254957]
21. Abe M, Harpel JG, Metz CN, Nunes I, Loskutoff DJ, RifkinDB. An assay for transforming growth factor-β using cells transfected with a plasminogen activator inhibitor-1 promoter-luciferase construct. Anal Biochem 1994;216:276–84. [PubMed: 8179182]
22. Montesano R, Orci L. Transforming growth factor β stimulates collagen-matrix contraction by fibroblasts: implications for wound healing. Proc Natl Acad Sci U S A 1988;85:4894–7. [PubMed: 3164478]
23. Lakos G, Takagawa S, Varga J. Animal models of scleroderma. Methods Mol Med 2004;102:377–93. [PubMed: 15286396]
24. Takagawa S, Lakos G, Mori Y, Yamamoto T, Nishioka K, Varga J. Sustained activation of fibroblast transforming growth factor-β/Smad signaling in a murine model of scleroderma. J Invest Dermatol 2003;121:41–50. [PubMed: 12839562]
25. Sime PJ, Xing Z, Graham FL, Csaky KG, Gauldie J. Adenovector-mediated gene transfer of active transforming growth factor-β1 induces prolonged severe fibrosis in rat lung. J Clin Invest 1997;100:768–76. [PubMed: 9259574]
26. Fang F, Shangguan AJ, Kelly K, Wei J, Gruner K, Ye B, et al. .Early growth response 3 (Egr-3) is induced by transforming growth factor-β and regulates fibrogenic responses. Am J Pathol 2013;183:1197–208. [PubMed: 23906810]
27. Milano A, Pendergrass SA, Sargent JL, George LK, McCalmont TH, Connolly MK, et al. Molecular subsets in the gene expression signatures of scleroderma skin. PLoS One 2008;3:e2696.
28. Pendergrass SA, Lemaire R, Francis IP, Mahoney JM, Lafyatis R, Whitfield ML. Intrinsic gene expression subsets of diffuse cutaneous systemic sclerosis are stable in serial skin biopsies. J Invest Dermatol 2012;132:1363–73. [PubMed: 22318389]
29. Huang da W, Sherman BT, Lempicki RA. Systematic and integrative analysis of large gene lists using DAVID bioinformatics resources. Nat Protoc 2009;4:44–57. [PubMed: 19131956]
30. Eisen MB, Spellman PT, Brown PO, Botstein D. Cluster analysis and display of genome-wide expression patterns. Proc Natl Acad Sci U S A 1998;95:14863–8. [PubMed: 9843981]

Author Manuscript Author Manuscript Author Manuscript Author Manuscript

31. Liu Y, Hayes DN, Nobel A, Marron JS. Statistical significance of clustering for high-dimension, low-sample size data. J Am Stat Assoc 2008;103:1281–93.
32. Steinhagen F, Meyer C, Tross D, Gursel M, Maeda T, Klaschik S, et al. Activation of type I interferon-dependent genes characterizes the “core response” induced by CpG DNA. J Leukoc Biol 2012;92:775–85. [PubMed: 22750547]
33. Stunz LL, Lenert P, Peckham D, Yi AK, Haxhinasto S, Chang M, et al. Inhibitory oligonucleotides specifically block effects of stimulatory CpG oligonucleotides in B cells. Eur J Immunol 2002;32:1212–22. [PubMed: 11981808]
34. Latz E, Schoenemeyer A, Visintin A, Fitzgerald KA, Monks BG, Knetter CF, et al. TLR9 signals after translocating from the ER to CpG DNA in the lysosome. Nat Immunol 2004;5:190–8. [PubMed: 14716310]
35. Kim YM, Brinkmann MM, Paquet ME, Ploegh HL. UNC93B1 delivers nucleotide-sensing toll-like receptors to endolysosomes. Nature 2008;452:234–8. [PubMed: 18305481]
36. Kyle RA, Rajkumar SV. Multiple myeloma. N Engl J Med 2004; 51:1860–73.
37. Lee AH, Iwakoshi NN, Anderson KC, Glimcher LH. Proteasome inhibitors disrupt the unfolded protein response in myeloma cells. Proc Natl Acad Sci U S A 2003;100:9946–51. [PubMed: 12902539]
38. Hirai M, Kadowaki N, Kitawaki T, Fujita H, Takaori-Kondo A,Fukui R, et al. Bortezomib suppresses function and survival of plasmacytoid dendritic cells by targeting intracellular trafficking of Toll-like receptors and endoplasmic reticulum homeostasis. Blood 2011;117:500–9. [PubMed: 20956804]
39. Loiarro M, Sette C, Gallo G, Ciacci A, Fanto N, Mastroianni D, et al. Peptide-mediated interference of TIR domain dimerization in MyD88 inhibits interleukin-1-dependent activation of NF-κB. J Biol Chem 2005;280:15809–14.
40. Kirillov V, Siler JT, Ramadass M, Ge L, Davis J, Grant G, et al. Sustained activation of toll-like receptor 9 induces an invasive phenotype in lung fibroblasts: possible implications in idiopathic pulmonary fibrosis. Am J Pathol 2015;185:943–57. [PubMed: 25660181]
41. Ewald SE, Lee BL, Lau L, Wickliffe KE, Shi GP, Chapman HA, et al. The ectodomain of Toll-like receptor 9 is cleaved to generate a functional receptor. Nature 2008;456:658–62. [PubMed: 18820679]
42. Park B, Brinkmann MM, Spooner E, Lee CC, Kim YM, Ploegh HL. Proteolytic cleavage in an endolysosomal compartment is required for activation of Toll-like receptor 9. Nat Immunol 2008;9:1407–14. [PubMed: 18931679]
43. Trujillo G, Meneghin A, Flaherty KR, Sholl LM, Myers JL, Kazerooni EA, et al. TLR9 differentiates rapidly from slowly progressing forms of idiopathic pulmonary fibrosis. Sci Transl Med 2010;2:57ra82.
44. Mathes AL, Rice L, Affandi AJ, DiMarzio M, Rifkin IR, Stifano G, et al. CpGB DNA activates dermal macrophages and specifically recruits inflammatory monocytes into the skin. Exp Dermatol 2015;24:133–9. [PubMed: 25425469]
45. Hinz B, Phan SH, Thannickal VJ, Prunotto M, Desmouliere A, Varga J, et al. Recent developments in myofibroblast biology: paradigms for connective tissue remodeling. Am J Pathol 2012;180:1340–55. [PubMed: 22387320]
46. Mutlu GM, Budinger GR, Wu M, Lam AP, Zirk A, Rivera S, et al. Proteasomal inhibition after injury prevents fibrosis by modulating TGF-β(1) signalling. Thorax 2012;67:139–46. [PubMed: 21921091]
47. Folcik VA, Garofalo M, Coleman J, Donegan JJ, Rabbani E, Suster S, et al. Idiopathic pulmonary fibrosis is strongly associated with productive infection by herpesvirus saimiri. Mod Pathol 2014;27:851–62. [PubMed: 24232864]
48. Zhang Q, Raoof M, Chen Y, Sumi Y, Sursal T, Junger W, et al. Circulating mitochondrial DAMPs cause inflammatory responses to injury. Nature 2010;464:104–7. [PubMed: 20203610]
49. Oka T, Hikoso S, Yamaguchi O, Taneike M, Takeda T, Tamai T, et al. Mitochondrial DNA that escapes from autophagy causes inflammation and heart failure. Nature 2012;485:251–5. [PubMed: 22535248]

Author Manuscript Author Manuscript Author Manuscript Author Manuscript

50. Gazdhar A, Lebrecht D, Roth M, Tamm M, Venhoff N, Foocharoen C, et al. Time-dependent and somatically acquired mitochondrial DNA mutagenesis and respiratory chain dysfunction in a scleroderma model of lung fibrosis. Sci Rep 2014;4:5336. [PubMed: 24939573]
51. Shinohara ML, Lu L, Bu J, Werneck MB, Kobayashi KS, Glimcher LH, et al. Osteopontin expression is essential for interferon-α production by plasmacytoid dendritic cells. Nat Immunol 2006;7:498–506. [PubMed: 16604075]
52. Wu M, Schneider DJ, Mayes MD, Assassi S, Arnett FC, Tan FK, et al. Osteopontin in systemic sclerosis and its role in dermal fibrosis. J Invest Dermatol 2012;132:1605–14. [PubMed: 22402440]
53. Watanabe A, Hashmi A, Gomes DA, Town T, Badou A, Flavell RA, et al. Apoptotic hepatocyte DNA inhibits hepatic stellate cell chemotaxis via toll-like receptor 9. Hepatology 2007;46: 1509–18. [PubMed: 17705260]
54. Ilvesaro JM, Merrell MA, Swain TM, Davidson J, Zayzafoon M, Harris KW, et al. Toll like receptor-9 agonists stimulate prostate cancer invasion in vitro. Prostate 2007;67:774–81. [PubMed: 17373717]
55. Luckhardt TR, Coomes SM, Trujillo G, Stoolman JS, Vannella KM, Bhan U, et al. TLR9-induced interferon β is associated with protection from gammaherpesvirus-induced exacerbation of lung fibrosis. Fibrogenesis Tissue Repair 2011;4:18. [PubMed: 21810214]
56. Abu-Tair L, Axelrod JH, Doron S, Ovadya Y, Krizhanovsky V, Galun E, et al. Natural killer cell-dependent anti-fibrotic pathway in liver injury via Toll-like receptor-9. PLoS One 2013;8:e82571.
57. Ito T, Schaller M, Raymond T, Joshi AD, Coelho AL, FrantzFG, et al. Toll-like receptor 9 activation is a key mechanism for the maintenance of chronic lung inflammation. Am J Respir Crit Care Med 2009;180:1227–38. [PubMed: 19797157]
58. Shen Y, Ichino M, Nakazawa M, Minami M. CpG oligodeoxynucleotides prevent the development of scleroderma-like syndrome in tight-skin mice by stimulating a Th1 immune response. J Invest Dermatol 2005;124:1141–8. [PubMed: 15955088]
59. Volpi C, Fallarino F, Pallotta MT, Bianchi R, Vacca C, Belladonna ML, et al. High doses of CpG oligodeoxynucleotides stimulate a tolerogenic TLR9-TRIF pathway. Nat Commun 2013;4:1852. [PubMed: 23673637]
60. Hennessy EJ, Parker AE, O'Neill LA. Targeting Toll-like receptors: emerging therapeutics? Nat Rev Drug Discov 2010;9:293–307. [PubMed: 20380038]

Author Manuscript Author Manuscript Author Manuscript Author Manuscript

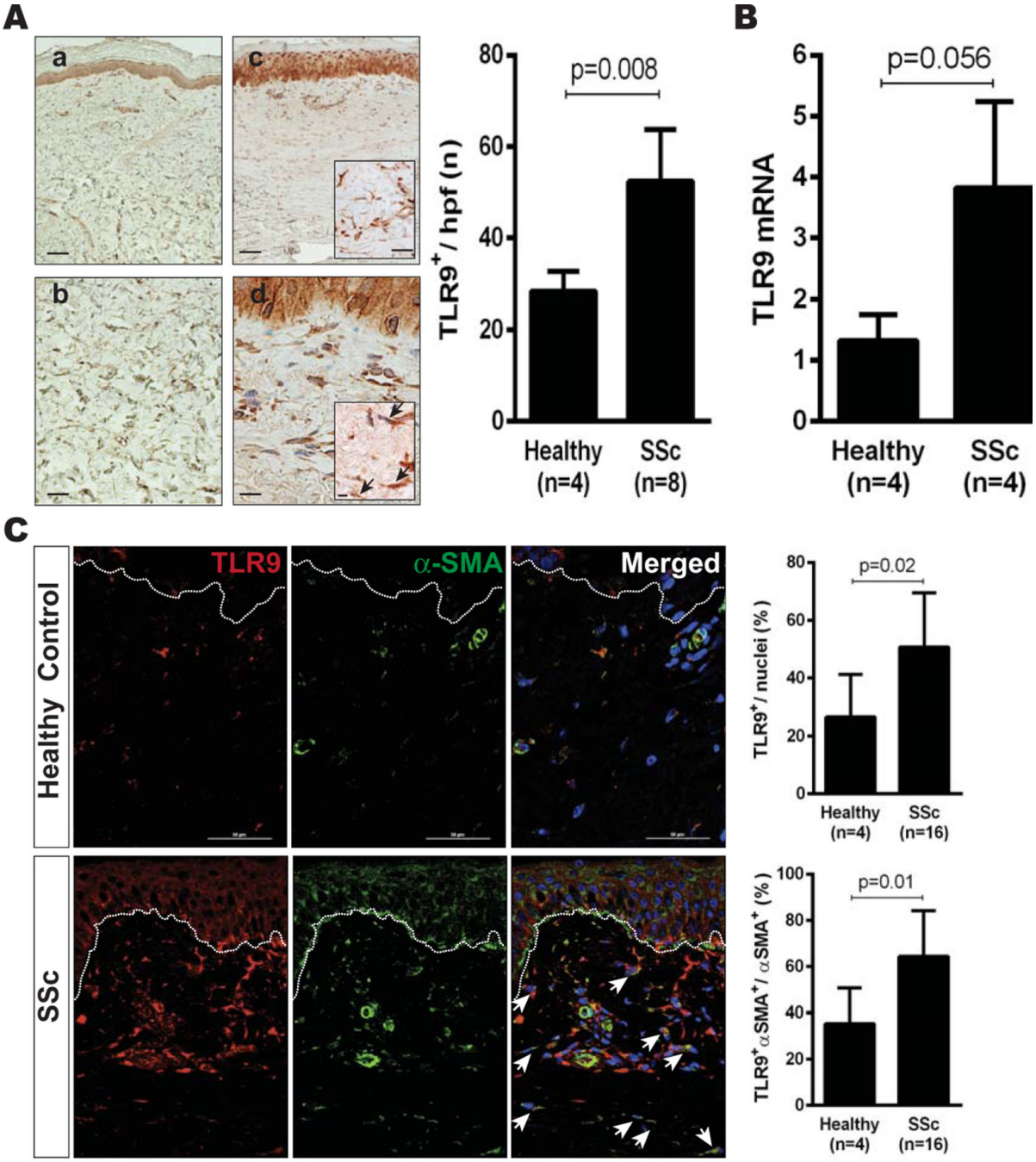

Figure 1.

Elevated Toll-like receptor 9 (TLR9) expression in systemic sclerosis (SSc). **A**, Left, Representative photomicrographs showing TLR9 expression in skin biopsy specimens obtained from healthy control subjects (**a** and **b**) and SSc patients (**c** and **d**), as determined by immunohistochemical analysis. **Arrows** indicate TLR9-positive cells. Bars in **a** and **c** = 25 μm; bars in **b**, boxed area in **c**, and **d** = 100 μm; bar in boxed area in **d** = 200 μm. Right, Quantification of TLR9-positive cells in the dermis. Values are the mean ± SD (5 high-power fields [hpf] per subject). **B**, TLR9 mRNA expression in confluent cultures

Author Manuscript Author Manuscript Author Manuscript Author Manuscript

of skin fibroblasts, as determined by real-time quantitative polymerase chain reaction. Values are the mean ± SD of triplicate determinations. **C**, Left, Representative double-label immunofluorescence microscopic images of skin biopsy specimens stained with antibodies to TLR9 (red) and α-smooth muscle actin (α-SMA) (green). Nuclei were stained with DAPI (blue). Dotted lines indicate the border between the epidermis and dermis. Bars = 50 μm. **Arrows** indicate double-positive cells. Right, Quantification of TLR9-positive and TLR9/α-SMA–double-positive cells in the dermis. Values are the mean ± SD (3 hpf per subject).

Author Manuscript Author Manuscript Author Manuscript Author Manuscript

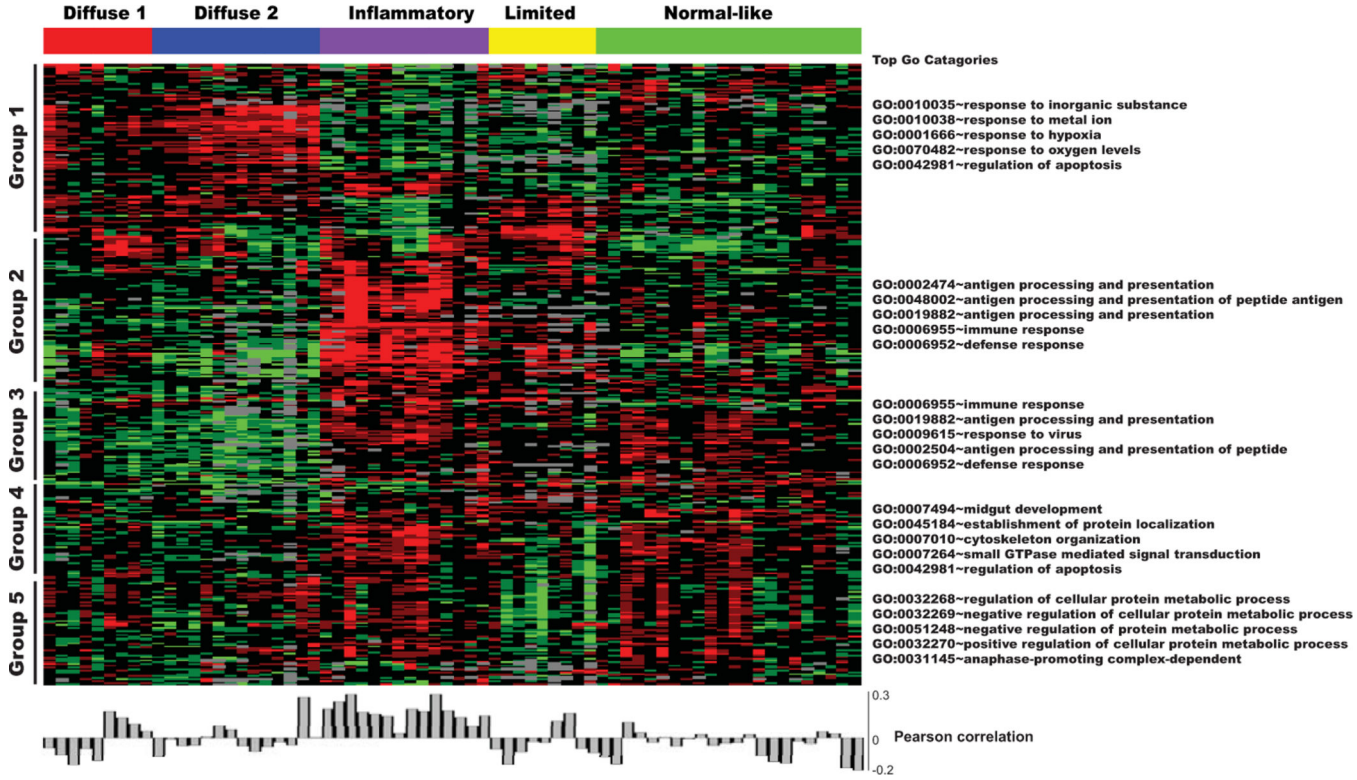

Figure 2.

TLR9-responsive gene signature in SSc skin biopsy specimens. An experimentally derived 314-gene TLR9 signature (GEO accession no. GSE30849) (23) was compared with SSc skin biopsy gene expression data (GEO accession nos. GSE9285 and GSE32413) (24,25). Heatmap shows groups of genes clustering hierarchically (black bars); the 5 most highly represented Gene Ontology (GO) terms can be seen alongside each cluster (right). Pearson's correlation of the TLR9 gene signature in each biopsy specimen is shown below heatmap. See Figure 1 for other definitions.

Author Manuscript Author Manuscript Author Manuscript Author Manuscript

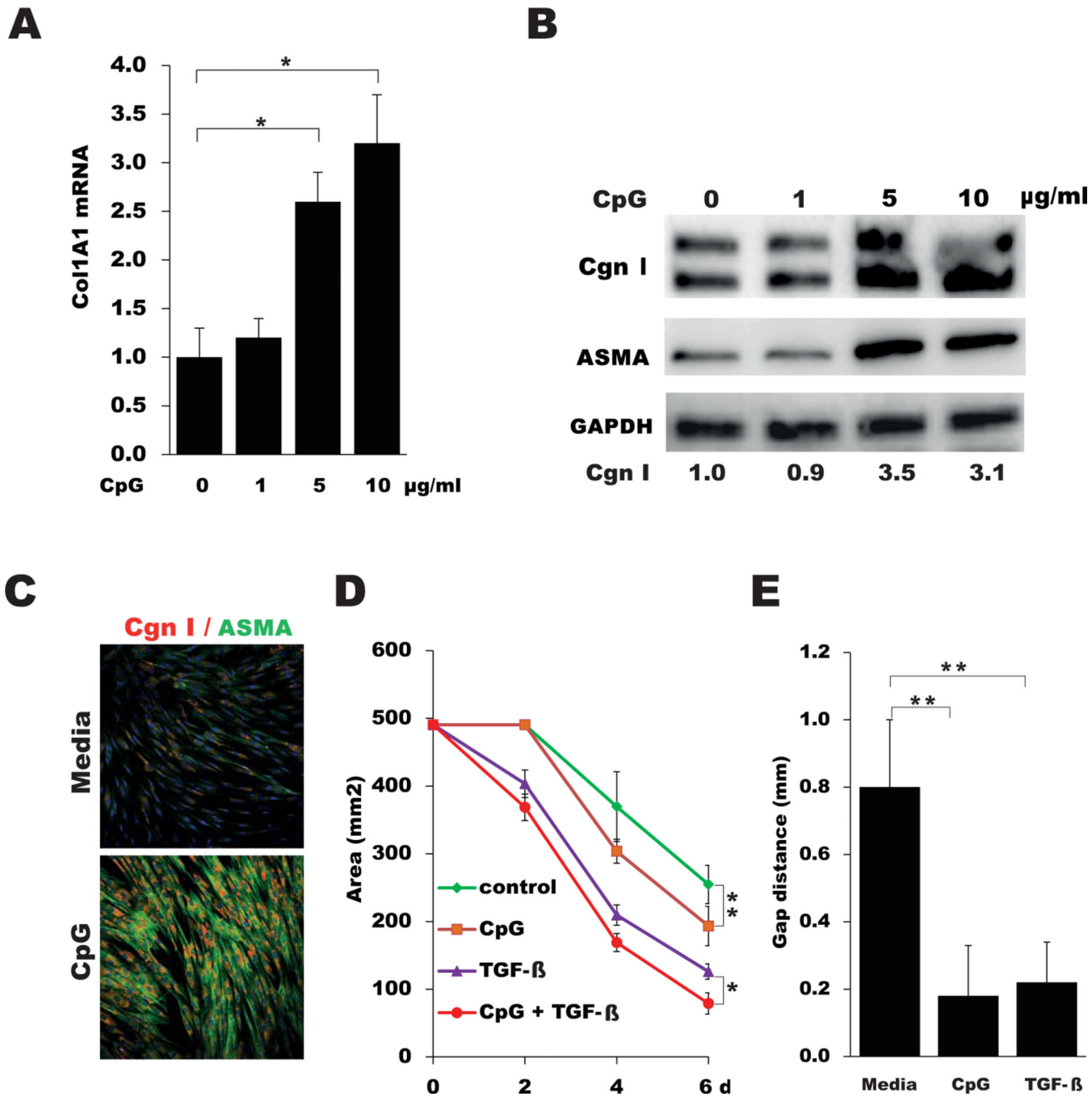

Figure 3.

Type A CpG elicits fibrotic responses in fibroblasts. **A**, Total COL1A1 mRNA in confluent skin fibroblasts incubated with the indicated concentrations of CpG, as determined by real-time quantitative polymerase chain reaction. Values are the mean ± SEM of triplicate determinations and are representative of 3 independent experiments. **B**, Western blot analysis of whole cell lysates, using antibodies to type I collagen (Cgn I), ASMA, and GAPDH. Band intensities are shown below each lane. Representative immunoblots are shown. **C**, Representative immunofluorescence microscopic images of fibroblasts

Author Manuscript Author Manuscript Author Manuscript Author Manuscript

immunostained with antibodies to ASMA (green) or type I collagen (red). Nuclei were stained with DAPI (blue). Original magnification × 200. **D**, Diameters of type I collagen gels seeded with fibroblasts and incubated in medium with CpG and transforming growth factor β (TGFβ), as measured on the indicated days (d). Values are the mean ± SEM of triplicate determinations. **E**, Fibroblast migration following incubation in medium with CpG or TGFβ for 24 hours, as determined using wound-healing assays. Values are the mean ± SEM of triplicate wells. * = $P < 0.05$; ** = $P < 0.01$.

Author Manuscript Author Manuscript Author Manuscript Author Manuscript

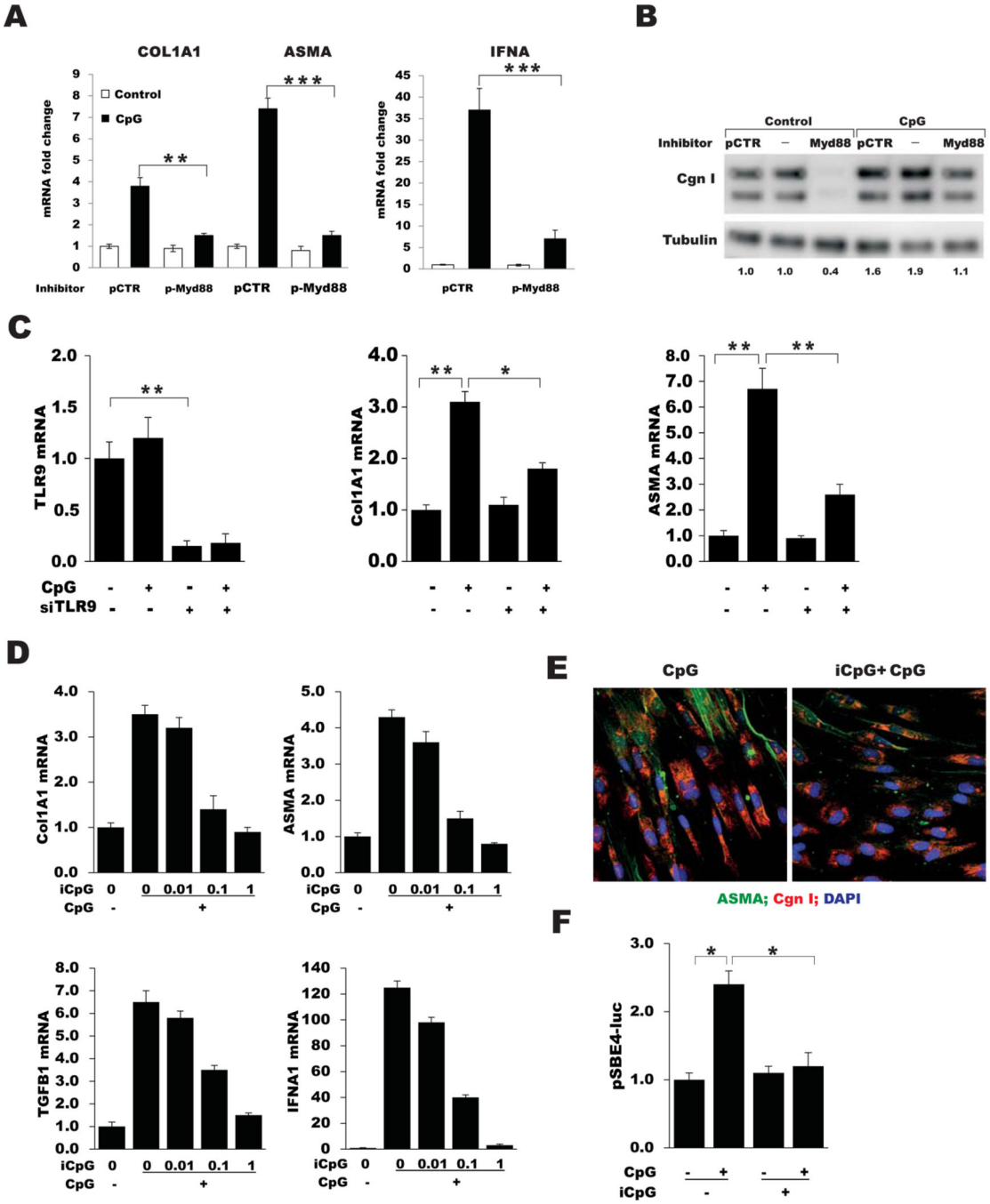

Figure 4.

CpG-induced fibrotic responses are Toll-like receptor 9 (TLR9) dependent. **A**, Fold changes in COL1A1, ASMA, and IFNA expression in skin fibroblast cultures pretreated with peptide myeloid differentiation factor 88 (pMyD88) and peptide control (pCTR), as determined by real-time quantitative polymerase chain reaction (qPCR). Values are the mean ± SEM of triplicate determinations. **B**, Western blot analysis of whole cell lysates, using antibodies to type I collagen and α-tubulin. Band intensities are shown below each lane. Representative immunoblots are shown. **C**, TLR9, COL1A1, and ASMA mRNA expression

Author Manuscript Author Manuscript Author Manuscript Author Manuscript

in skin fibroblasts transiently incubated with TLR9 small interfering RNA (siTLR9) or scrambled control siRNA in parallel and incubated with CpG, as determined by qPCR. Values are the mean ± SEM of triplicate determinations. **D**, COL1A1, ASMA, TGFB1, and IFNA1 mRNA expression in fibroblasts pretreated with pMyD88 or inhibitory CpG (iCpG) followed by CpG, as determined by qPCR. Values are the mean ± SEM of triplicate determinations. **E**, Representative immunofluorescence microscopic images of fibroblasts stained with antibodies to ASMA (green), type I collagen (Cgn I; red), and DAPI (blue). Original magnification × 100. **F**, Luciferase activity in cell lysates after pretreatment with iCpG, followed by CpG. Values are the mean ± SEM of triplicate determinations and are representative of 3 independent experiments. * = $P < 0.05$; ** = $P < 0.01$; *** = $P < 0.001$.

Author Manuscript Author Manuscript Author Manuscript Author Manuscript

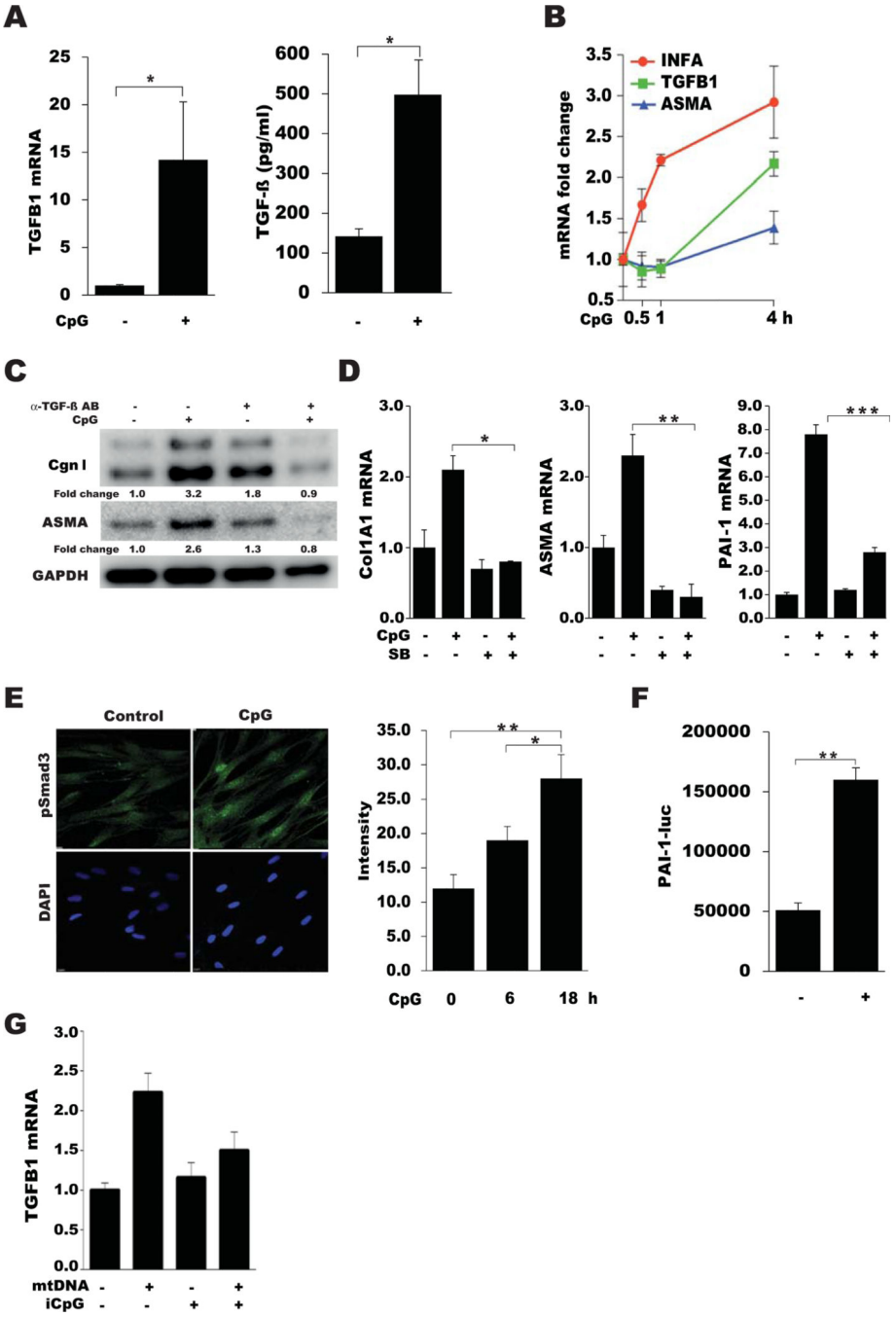

Figure 5.

TLR9-mediated fibrotic responses are transforming growth factor β (TGFβ) dependent. **A–E**, Confluent skin fibroblasts were incubated in media with CpG alone or with TGFβ. **A**, Left, Levels of TGFB1 mRNA as determined by qPCR. Values are the mean ± SEM of triplicate experiments. Right, Levels of TGFβ secreted in medium, as determined by enzyme-linked immunosorbent assay. **B**, Fold changes in mRNA levels at the indicated time points. Values were normalized to GAPDH mRNA values and are the mean ± SEM of triplicate determinations. **C**, Western blot analysis of whole cell lysates, treated

Author Manuscript Author Manuscript Author Manuscript Author Manuscript

with or without anti-TGFβ antibodies (AB). Representative immunoblots are shown. **D**, Expression of COL1A1, ASMA, and PAI1 mRNA in cultures preincubated with or without SB431542 (SB) for 60 minutes, as determined by qPCR. Values are the mean ± SEM of triplicate determinations. **E**, Left, Representative immunofluorescence microscopic images of confluent skin fibroblasts stained with anti-pSmad3 antibodies (green) and DAPI (blue), in the absence or presence of CpG. Original magnification × 100. Right, Quantification of nuclear pSmad3 phosphorylation at different time points. Values are the mean ± SD of 5 randomly selected high-power fields. **F**, Plasminogen activator inhibitor (PAI-1)–Luc activity in cell-free conditioned medium from fibroblasts incubated with or without CpG. Values are the mean ± SEM of triplicate determinations and are representative of 3 independent experiments. **G**, Expression of TGFB1 mRNA in fibroblasts incubated with mitochondrial DNA (mtDNA) in the absence or presence of iCpG. Values are the mean ± SEM. * = $P < 0.05$; ** = $P < 0.01$; *** = $P < 0.001$. See Figure 4 for other definitions.

Author Manuscript Author Manuscript Author Manuscript Author Manuscript

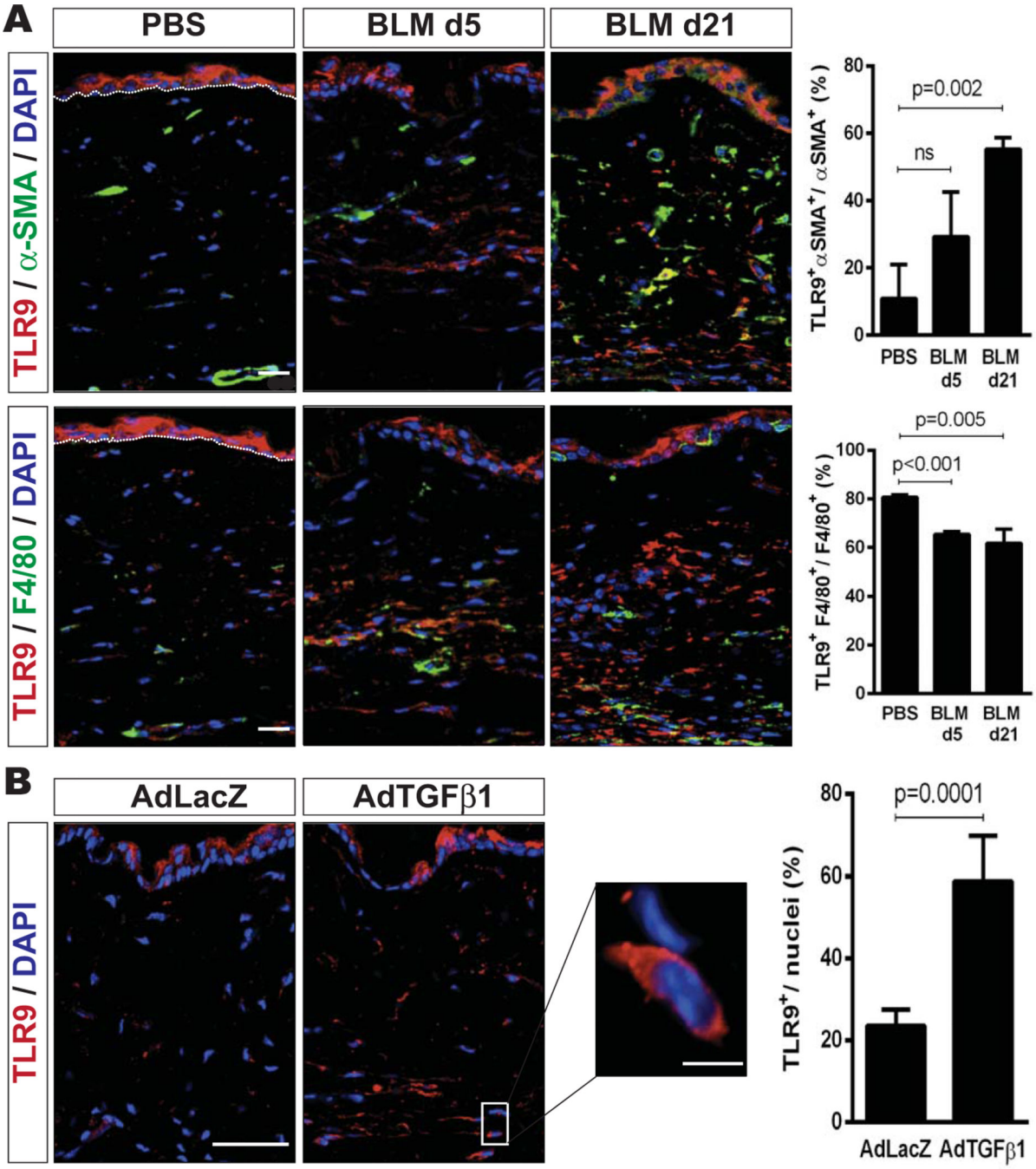

Figure 6.

Skin fibrosis in murine scleroderma is accompanied by up-regulated Toll-like receptor 9 (TLR9) expression. **A**, Left, Representative immunofluorescence microscopic images of lesional skin harvested on day 5 (d5) or day 21 from mice that received daily subcutaneous injections of bleomycin (BLM) or phosphate buffered saline (PBS), showing staining for TLR9 (red), α-smooth muscle actin (α -SMA) (green), or F4/80 (green). Nuclei were stained with DAPI (blue). Bars = 20 μm. Right, Quantification of cells double-positive for TLR9 and α -SMA (top) or TLR9 and F4/80 (bottom). Values are the mean ± SEM

Author Manuscript Author Manuscript Author Manuscript Author Manuscript

percentage. **B**, Left, Representative immunofluorescence microscopic images of lesional skin harvested on day 42 from mice that received a single injection of AdTGFβ1 or AdLacZ, showing staining for TLR9. Nuclei were stained with DAPI. Bar = 20 μm; bar in higher-magnification view of boxed area = 10 μm. Right, Quantification of the number of TLR9-positive cells per nuclei in 3 high-power fields per mouse. Values are the mean ± SEM percentage (≥3 mice per treatment group).